FINGERPRINT-INSPIRED TRIBOELECTRIFIC SLIDING SENSOR

Haotian Chen[1, †], Zijian Song[2, †], Yu Song[2], Xuexian Chen[1], Liming Miao[2], Zongming Su[2], and Haixia Zhang[1,2,]*

[1]Academy for Advanced Interdisciplinary Studies, Peking University, CHINA

[2]Institute of Microelectronics, Peking University, CHINA

ABSTRACT

Inspired by the structure of human fingerprint, a novel sliding sensor composed of four spiral and alternate electrodes is presented in this work. Based on triboelectric and electrostatic induction effects, four electrodes generate voltage signals one after another when an external object move across the surfacce. According to this mechanism, sequence of four signals can not only figure out sliding direction but also detect displacement and speed of the sliding object by calculating the number of signal valleys and corresponding time interval. The sensor, which is fabricated by carbon nanotube and polydimethylsiloxane (CNT-PDMS) composite electrode on elastomer substrate, has very good stretchability enabling its easy coverage on robot hand and detection of sliding motion on irregular surfaces.

INTRODUCTION

Human skin is a remarkable organ that cover the whole body with the ability of multi-stimuli detection such as pressure, shear and temperature. Inspired from this, plenty of stretchable electronics have triggered significant technological progress in lots of field such as wearable electronics[1,2,3] and smart robot[4,5].

Fingerprint, which has the highest sensitivity[6] in human body due to its delicate structure, has drawn a lot of attentions in electronic skin areas, in which researcher intended to enhance the performance of stretchable sensors like pressure sensing and sliding detection[7,8].

What's more, a new sensing mechanism named triboelectric nanogenerator (TENG), which is dependent on triboelectric effect and electrostatic induction effect, has made lots of progress in both energy harvesting[9,10] and self-power sensing[11,12] in recent years. Four different working mechanisms[13] including contact-separate mode, sliding mode, single-friction-surface mode and freestanding mode, have been proposed to ensure the TENG can operate smoothly in almost any conditions. In addition, due to its the simple structure, low-cost fabrication process and easy collection of signal, TENG is applied in plenty of fields working as an active sensor[14].

In this work, we demonstrate a fingerprint-inspired TENG sliding sensor made from carbon nanotube-polydimethylsiloxane (CNT-PDMS), enabling its flexibility and stretchablity. What's more, it is the first time that a digital method to detect sliding direction and speed at the same time without external battery is proposed. Apart from that, according to the frequency of TENG output rather than amplitude, this sensor can work stably without influence from environment such as humidity.

FABRICATION

Figure 1(a) is a demonstration of a real human finger, from which we can see many circle-shaped ridges on it. The ridges is responsible for roughness sensing. Inspiored from this unique structure, we design a device consisting of a PDMS substrate and four spiral electrodes, each of which works as a single-friction-surface TENG (STENG), respectively. The pattern of electrodes is carefully designed to ensure no matter which direction an external object sliding across the surface of the sensor, each STENG can be activate the electrodes one by one. Moreover, the response sequence of TENGs is dependent on the sliding direction, which provide a way for direction detection.

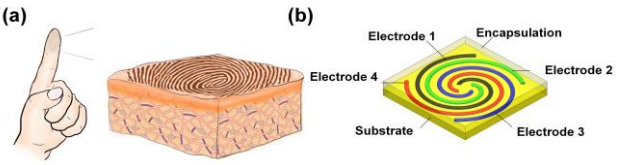

Figure 1. (a) Structure of human fingerprint. (b) Schematic diagram of the device containing four spiral electrodes.

CNTs was purchased from Boyu Co.,China with length of 10μm. Firstly, 5g CNTs were mixed with PDMS base (Dow Corning, Sylgard 184) at the mass fraction we needed. 20ml toluene was added into the mixture of CNT and PDMS with volumn ratio of 4:1 to make the CNT disperse uniformly in PDMS. Then the mixture of these three materials was stirred for 6h using magnetic stirring apparatus. After CNTs was well mixed into PDMS with the help of toluene, the mixture was poured into an evaporating dish to evaporate residual toluene. The cross-linking agent of PDMS can not be added until the toluene was thoroughly removed. Then, the prepared CNT-PDMS together with its cross-linking agent was cast into a 3D-printed mold and then baked at 70 °C for 2 hours. After the spiral CNT-PDMS was solidified, pure liquid PDMS was poured onto the electrodes serving as a substrate and solidified with the CNT-PDMS together. In this way, the substrate was bonded with the electrodes and can be peel off together from the mold. The resistance of CNT-PDMS can be modulated by controlling the mass ratio of CNT and PDMS. Key structural parameters of sliding sensor such as width of electrode (w), distance between neighboring electrodes (g) and the height of electrode (h) are shown in Table 1.

The coin-sized dimension of the sensor (Figure 3a) enable its broad integration in many fields. The small size and thin thickness of the sensor enable the sensor can be easily integrated on many irregular surfaces.

As a demonstration, the sensor is covered on a finger of a robot hand (Figure 3b). As it is fabricated with soft materials, the sensor can be easily covered on the finger surfaces, which broaden its application field.

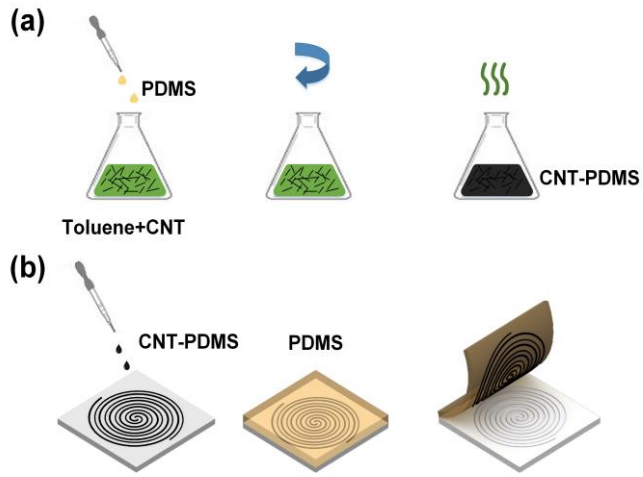

Figure 2. (a) Preparation process of CNT-PDMS. (b) Fabrication process of the device.

Table 1. Parameters of the sensor

Width of electrode (w)	*1mm*
Gap between electrodes(g)	*1mm*
Height of electrode (h)	*200um*

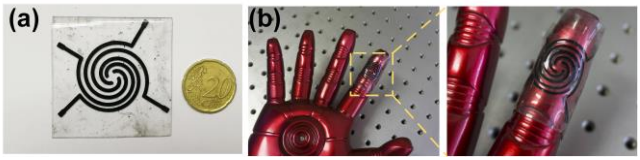

Figure 3. (a) Photograph of the fabricated device. (b) Robotic hand equipped with this sensor showing its flexibility.

WORKING PRINCIPLE

Working principle of this sensor is shown in Figure 4. When an outer object contacts the sensor, a charge separation will be generated due to the contact electrification effect (Figure 4(a)-4(b))[13].

For convenience, four electrodes are marked in different colors, red (E1), black (E2), green (E3) and blue (E4), respectively. As the outer object with electrostatic charges moves, electric potential will be redistributed among the four electrodes. Taking one direction as example, when the outer object move close to E1, much more positive charges will be induced on E1 compared with the other three electrodes due to the electrostatic induction effect. In this way, a higher potential is produced on E1 shown in Figure 4c. As the outer object continues to move, E2 will induce more positive charges while the number of positive charges on E1 decreases dramatically. So the potential of E2 gets to the highest among the four electrodes (Figure 4d), thus generating a current flowing from the electrode to the ground. Then the outer object goes on to move, E3 gets the highest potential as shown in Figure 4e. Similar potential distribution can be inferred when the object moves E4 as shown in Figure 4e-4f.

SIMULATION RESULT

Finite element method (FEM) is carried out to simulate the output of the whole sensor. Four spiral electrodes are specially designed to generate voltages one by one. What's more, the outmost part of electrode is different at each sides of the square substrate, the sequence of signals is also different when the object slides from different directions. As the outer object moves along -X direction as shown in Figure 5a, all of the voltages from 4 electrodes goes down until it definitely located above the E1, where the voltage of E1 gets the lowest. As the object continues to move along this direction, the voltage of E1 begins to increase while the other three voltages from E2-E4 continue to decrease. Similarly, the voltage of E2 reaches the lowest when the object moves above E2. When the object moves to the center of the sensor, E3 and E4 get to the lowest voltages one after another. By detecting the order of the four electrodes get the lowest voltage, which is '1234' in this condition, the sliding direction can be inferred.

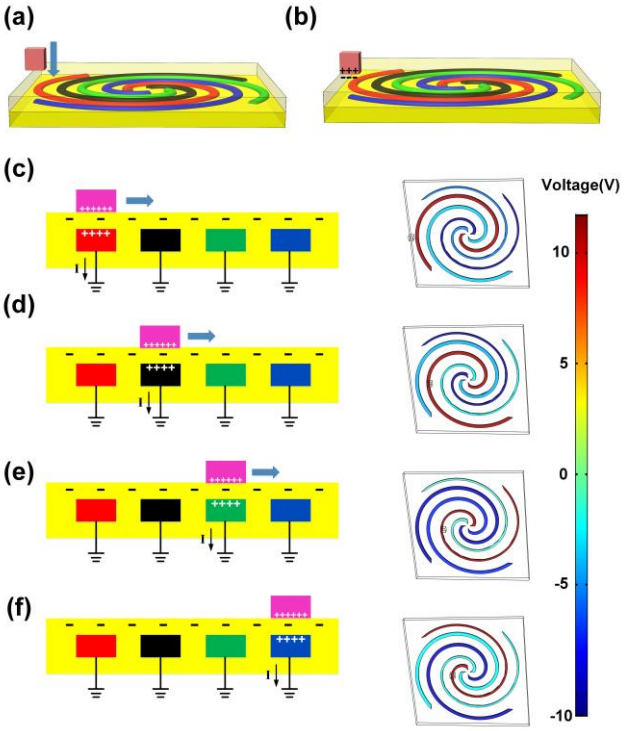

Figure 4. (a)(b) Process of contact electrification. (c)-(f)Working principle of this device together with the simulation result indicating how the potential changes.

In the similar way, when the object moves along +Y, +X and –Y directions, the corresponding voltage sequence is '2341', '3412' and '4123', respectively. By increasing the number of electrode in the sensor, the sliding direction can be increase from four to more directions.

Besides the direction detection, the sensor can also be responsible for displacement detection according to the number of voltage valleys (*N*) and structural parameters of width of the electrode *(w)* and gap between nearest two electrodes *(g)* by calculating *N*(w+g)*. What's more, the sliding speed can also be inferred from the displacement calculated above and the time intervals (*t*) between two valleys.

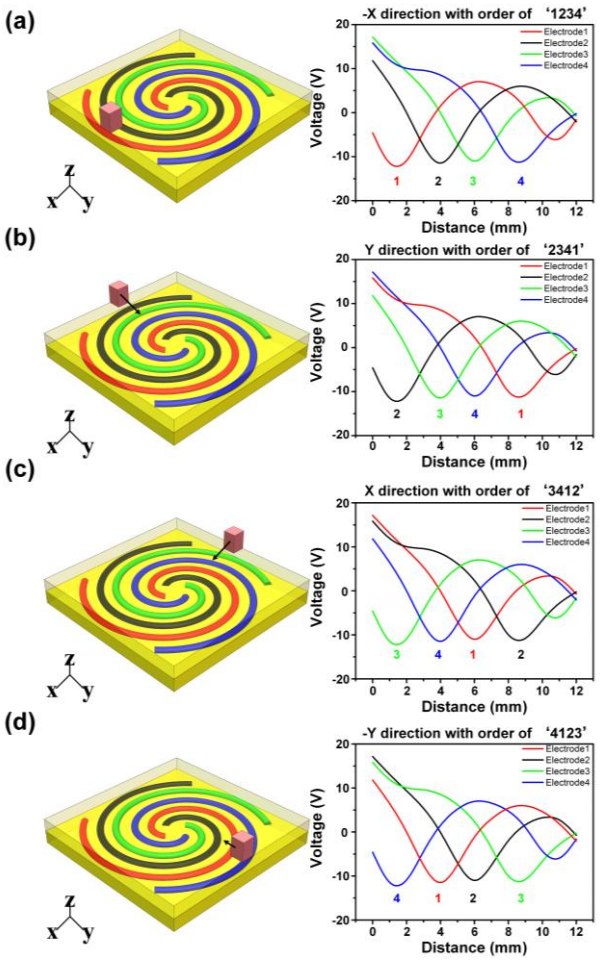

Figure 5. Simulation results showing how to detect sliding motion from different directions with this sensor and how to calculate movement speed.

RESULT AND DISCUSSION

In order to demonstrate the practical performance of this fingerprint-shaped sliding sensor, human finger is adopted as the moving object to move across the sliding sensor and the test results from four directions are demonstrated in Figure 6.

Figure 6a demonstrates the movement of human finger along the –X direction with sequence of '1234'. From the waveform, it can be inferred that at the beginning of the movement, the speed is as fast as *(w+g)/t=2mm/0.4s=5mm/s* due to the short time interval between the valleys of E1 and E2. After the finger gets to E3, the speed is dramatically decease to *(w+g)/t=2mm/2.3s=0.87mm/s.* In this way, this fingerprint-shaped STENG can not only tell the moving direction but also reflect the moving details such as speed at some specific location interval.

The movement of human finger along the +Y direction is demonstrated in Figure 6b. The speed in this direction is stable around 4mm/s. Similar movements along +X and –Y directions are shown in Figure 6c and Figure 6d, respectively. No matter in what direction, both the displacement and speed can be calculated from analyzing the waveform.

One of the most significant feature of this STENG based sliding sensor is that it is dependent on the frequency rather than the amplitude of the output, which provide an efficient way of sliding detection no matter in what condition. Amplitude of TENG is usually affected by a lot of environmental factors such as humidity. By utilizing frequency, the output can also reflect the characteristics of movement although the amplitude may be different. The peak-to-peak voltage in Figure 6(a) is around 0.9V while the value in Figure 6(b) is only 0.6V. However, this difference will not affect the result of displacement and speed, which enhance the reliability of the sensor greatly.

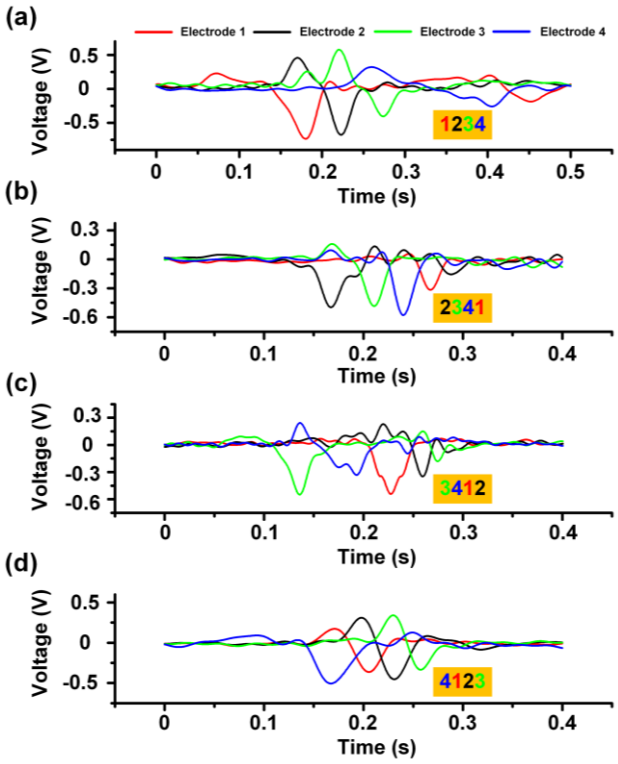

Figure 6. Experimental data demonstrating the sensor can effectively detect sliding move in different directions at different speeds.

CONCLUSIONS

In summary, we fabricate a fingerprint-shaped sliding sensor based on the triboelectric effect and electrostatic effect, which can not only distinguish the sliding direction but also detect the displacement and speed at the same time. STENG provides a simple but effective way to detect the movement without external batteries. By designing four spiral electrodes, each of which has the same shape and thread pitch but different initial positions, four separate STENGs can work sequentially when an outer object moves across the surface of the sensor. Due to the different initial positions of the four electrodes, the sequence of the generated voltage can reflect the moving directions. Besides the detection of sliding direction, sliding speed can also be detected by calculating the number of voltage valleys and time interval. Both of simulating results and

experimental results prove that this sensor can effectively operate based on the triboelectric effect. What's more, different from traditional TENG sensors based on the amplitude which often are susceptible to outer environment factors such as humidity, this frequency-based detective method provide a much more reliable results compared to the amplitude-based devices.

ACKNOWLEDGEMENTS

This work is supported by the National Natural Science Foundation of China (Grant No. 61674004), and the Beijing Natural Science Foundation of China (Grant No. 4141002).

REFERENCE

[1] D. Kim, N. Lu, R. Ma, et al. Epidermal electronics[J]. science, 2011, 333(6044): 838-843.
[2] J. Park, Y. Lee, J. Hong, et al. Giant tunneling piezoresistance of composite elastomers with interlocked microdome arrays for ultrasensitive and multimodal electronic skins[J]. ACS nano, 2014, 8(5): 4689-4697.
[3] Z. Su, H. Wu, H. Chen, et al. Digitalized Self-Powered Strain Gauge for Static and Dynamic Measurement[J]. Nano Energy, 2017.
[4] M. Hammock, A. Chortos, B. Tee, et al. 25th anniversary article: the evolution of electronic skin (e-skin): a brief history, design considerations, and recent progress[J]. Advanced Materials, 2013, 25(42): 5997-6038.
[5] R. Dahiya, P. Mittendorfer, M. Valle, et al. Directions toward effective utilization of tactile skin: A review[J]. IEEE Sensors Journal, 2013, 13(11): 4121-4138.
[6] A. Vallbo, S. Johansson. Properties of cutaneous mechanoreceptors in the human hand related to touch sensation[J]. Hum Neurobiol, 1984, 3(1): 3-14.
[7] H. Chen, L. Miao, Z. Su, et al. Fingertip-inspired electronic skin based on triboelectric sliding sensing and porous piezoresistive pressure detection[J]. Nano Energy, 2017, 40: 65-72.
[8] H. Chen, Z. Su, Song Y, et al. Omnidirectional Bending and Pressure Sensor Based on Stretchable CNT-PU Sponge[J]. Advanced Functional Materials, 2017, 27(3).
[9] F. Fan, W. Tang, Z. Wang. Flexible Nanogenerators for Energy Harvesting and Self-Powered Electronics[J]. Advanced Materials, 2016, 28(22): 4283-4305.
[10] X. Cheng, L. Miao, Z. Su, et al. Controlled fabrication of nanoscale wrinkle structure by fluorocarbon plasma for highly transparent triboelectric nanogenerator[J]. Microsystems & Nanoengineering, 2017, 3: 16074.
[11] S. Wang, L. Lin, Z. Wang. Triboelectric nanogenerators as self-powered active sensors[J]. Nano Energy, 2015, 11: 436-462.
[12] M. Shi, J. Zhang, H. Chen, et al. Self-powered analogue smart skin[J]. ACS nano, 2016, 10(4): 4083-4091.
[13] G. Zhu, B. Peng, J. Chen, et al. Triboelectric nanogenerators as a new energy technology: From fundamentals, devices, to applications[J]. Nano Energy, 2015, 14: 126-138.
[14] B. Meng, W. Tang, Z. Too, et al. A transparent single-friction-surface triboelectric generator and self-powered touch sensor[J]. Energy & Environmental Science, 2013, 6(11): 3235-3240.

CONTACT

*H.X. Zhang, Tel: +86-10-62767742;
zhang-alice@pku.edu.cn
†These authors contribute equally.